Seismic Vulnerability of URM Structures based on a Discrete Macro-Element Modeling (DMEM) Approach

César Chácara[1,2], Francesco Cannizzaro[3], Bartolomeo Pantò[3], Ivo Caliò[3], Paulo B. Lourenço[2]

[1] Pontificia Universidad Católica del Perú, San Miguel Lima 32, Lima, Perú. Phone: +51 16262000, E-mail: c.chacara@pucp.pe

[2] ISISE, University of Minho, Department of Civil Engineering, Azurém, 4800-058 Guimarães, Portugal. Phone: +351 253 510 200, fax: +351 253 510 217, E-mail: pbl@civil.uminho.pt

[3] University of Catania, Department of Civil Engineering and Architecture, 95125 Catania, Italy. Phone: +39 095 738 2275, fax: +39 095 738 2249, E-mail: francesco.cannizzaro@dica.unict.it, bpanto@dica.unict.it, icalio@dica.unict.it

1. Abstract

The assessment of the seismic vulnerability of unreinforced masonry (URM) structures based on numerical modeling constitutes a difficult task due to their complex behavior, especially in the nonlinear dynamic field, and the lack of suitable, low-demanding, computational tools. In the last decades, practical statistical tools for the derivation of fragility curves has been successfully proposed mainly with reference to framed structures. This approach has been adopted also for the seismic vulnerability assessment of masonry buildings focusing on the in-plane collapse mechanisms by means of equivalent frame models. Nevertheless, the lack of computationally effective tools which involve the interaction between in-plane and out-of-plane mechanisms makes the definition of fragility curve an arduous task when it comes to existing masonry structures without box behavior.

In this paper, a practical and thorough methodology for the assessment of the seismic vulnerability of URM buildings by means of analytical fragility curves is presented. This methodology presents some innovative features such as the definition of the limit states (LSs) and their corresponding capacity based on multi-directional pushover analyses, as well as the application of nonlinear dynamic analyses, performed using a discrete macro-element modelling approach capable of simulating the main in-plane and out-of-plane responses of URM structures with a reduced computational burden. The present investigation focuses on the application of this methodology for assessing the seismic vulnerability of a brick masonry structure characterized by a strong out-of-plane failure mechanism. After a fitting process, the fragility curves were compared to the ones obtained using expert-based approaches.

Keywords: Brick masonry structure, Multi-directional pushover analysis, Nonlinear dynamic analysis, Displacement capacity, Analytical fragility curves, HiStrA software.

1. Introduction

Masonry buildings constitute the most scattered low-rise structural typology in the world, mainly because of its economic affordability and constructive ease. In addition to residential buildings, the vast majority of heritage constructions, usually made of brick, stone or adobe, also belong to this structural typology. These structures are often located in areas with high seismic activity, and most of them were built without following specific seismic design standards. It is well-known that, besides being an important cause of human losses, earthquakes constitute a major threat involving the stability of this typology of structures. Therefore, the seismic vulnerability assessment of this structural typology is a relevant topic within the different fields concerning decision making, risk prediction and management of seismic hazard. Nevertheless, masonry structures present a response difficult to predict due to the high uncertainty associated with variables such as their mechanical, geometrical or structural parameters, or load conditions to which they are subjected to. Considering the high uncertainty of this type of buildings, deterministic approaches are less suitable for assessing the seismic vulnerability of URM structures. In this sense, stochastic-probabilistic methodologies are desirable to better understand the seismic vulnerability assessment of this type of structures [1].

Seismic vulnerability assessment is often performed using practical statistical tools such as fragility functions which allow the estimation of the probability of reaching or exceeding a limit state (LS) due to a given Intensity Measure (IM) [2]. Fragility functions can be defined following different approaches, namely expert-based, analytical, empirical and hybrid formulations [3]. The definition of fragility functions by means of expert-based formulations involves a substantial and detailed assessment of an estimate of damage level provided by a team of experts [4]. Nevertheless, due to the diverse individual experiences of the experts, damage estimates with a high level of consensus may not be reached, making this type of formulation somehow limited. On the other hand, empirical-based fragility functions involve a statistical elaboration of data obtained from post-earthquake surveys. This type of formulation is based on a more realistic source of information (such as structural

typologies, soil effects and site characteristics) allowing a more accurate assessment of the seismic vulnerability. Fragility functions derived from analytical formulations involve the development of structural models and the subsequent performing of numerical simulations. Even though this type of fragility functions may increase the reliability of the seismic vulnerability assessment by reducing the bias associated with expert-based formulations, its derivation still presents some important limitations. Sophisticated numerical tools require a significantly large computational burden and the extensive knowledge of input parameters. Furthermore, most simplified models currently used for the numerical simulations are not capable of providing a realistic prediction of the earthquake structural response since they neglect the interaction between in-plane and out-of-plane mechanisms.

Another important aspect that plays a fundamental role in the assessment of seismic vulnerability, based on nonlinear analyses, corresponds to the definition of appropriate IMs and LSs. Macroscale intensity measures as the Peak Ground Acceleration (PGA) constitute parameters commonly used for the derivation of fragility functions due to the simple physical meaning they provide [5]. Other parameters such as the peak ground velocity, the spectral acceleration or spectral displacement, the Arias and Housner intensities have been considered as IMs for seismic vulnerability assessment [6]. LSs are related to the response of a building, and they are commonly based on its structural performance. This performance is often related to interstory drifts formulations as specified in different codes or standards [7-11] or proposed by different authors [12-15]. The most common formulation for assessing the seismic vulnerability of masonry structures is based on the interstory drift capacity. As reported in the EC8-Part3 [9], the definition of this displacement-based formulation is associated with the type of mechanism governing the collapse of the structure. For instance, a lateral drift of 0.4% is proposed for a Significant Damage LS when the structure experiences a shear failure, and 0.8% (H_0/L) when the collapse is ruled by a flexural mechanism, being H_0 and L the distance between the contra-flexure point and the point in which the flexural capacity is attained, and the in-plane length of the wall, respectively. It is worth to note that similar failure mechanism-based procedures have been adopted

by additional standards such as Italian Code [11], FEMA 273 [7] and FEMA 306 [8]. A summary of the different interstory drift-based procedures and a detailed comparison can be found in the work presented by Petry and Beyer [16]. On the other hand, a multiscale approach was proposed in [17, 18] for the definition of LSs. This approach involves the structure performance assessment at three different levels: i) local, ii) global, and iii) macro-element. The application of this approach is mainly suitable for multistory masonry buildings in which the global behavior is most influenced by the in-plane response of masonry walls. The assessment of buildings characterized by flexible diaphragms or by the absence of diaphragms requires additional criteria. In this regard, the authors have proposed the application of macro block models in order to assess the out-of-plane mechanisms of this type of buildings and its integration with the multiscale approach.

Very few studies are devoted to the assessment of the seismic vulnerability of unreinforced masonry buildings based on fragility functions [19]. Rota, et al. [5] investigated the seismic vulnerability of some typical Italian masonry structures using empirical fragility functions. The derivation of such functions was based on post-earthquake damage data relative to 91,934 buildings, classified into twenty-three structural typologies, and the definition of five LSs in accordance with the European Macroseismic Scale [20]. The seismic vulnerability assessment required the formulation of Damage Probability Matrices for each structural typology and PGA interval. A similar investigation regarding Iranian buildings was carried out by Omidvar, et al. [21] in 2012.

The seismic vulnerability of masonry structures has also been investigated by means of analytical formulations and the use of simplified computational tools. For instance, Park, et al. [22] investigated the seismic vulnerability of low-rise URM buildings located in the central and southern regions of the US using simplified numerical models. In this sense, the walls loaded in the in-plane direction were modeled as an arrangement of nonlinear links in series, whereas the walls loaded in the out-of-plane direction and horizontal diaphragms were simulated as single nonlinear links. Four LSs together with their corresponding

150 interstory drift capacities were established in accordance with specifications
151 provided by HAZUS [23].
152 Pasticier, et al. [24] investigated the seismic vulnerability of a typical two-
153 story stone masonry building using an equivalent frame modeling approach,
154 performed with the software SAP2000 [25], consistent with the three LSs defined
155 in the EC8-Part3 [9]. The global behavior of the building was firstly investigated
156 through static pushover analyses. Subsequently, a simplified model of the
157 building's façade was subjected to Incremental Dynamic Analysis (IDA) based on
158 fourteen earthquake ground motion records with different scaling factors. In such
159 investigation, the uncertainty was focused on the PGA, which was also considered
160 as IM.
161 Asteris [14] defined specific damage states for the evaluation of the seismic
162 vulnerability of masonry structures. These states were used for the seismic
163 assessment of a Greek historical monastery [26]. In such investigation, fragility
164 curves were derived by means of FE numerical simulations. The seismic
165 vulnerability also involved the use of different restoration mortars in order to
166 determine the best alternative for strengthening purposes. The mortars were
167 obtained by means of an inverse engineering procedure aiming at assuring their
168 compatibility with the original constituent material [27]. Asteris, et al. [28] also
169 investigated the seismic vulnerability of historical masonry structures located in
170 Portugal, Cyprus and Greece. Numerical models of these masonry structures,
171 based on the FE method, were used for the generation of fragility curves. In a more
172 recent investigation, Asteris, et al. [1] presented a methodology for seismic
173 vulnerability assessment which involves activities such as geometrical
174 reconstruction, mechanical characterization, numerical modeling, definition of
175 seismic actions and failure criteria, application of strengthening techniques, and
176 derivation of fragility curves. The latter investigation also considered that the
177 limit states were based on a damage-based approach. The methodology was
178 applied to a set of masonry walls considering uncertainty related to tensile
179 strength, percentage of openings, and peak ground acceleration.
180 The seismic vulnerability of an Italian typological three-story masonry
181 building was assessed by Rota, et al. [19]. An equivalent frame computational

model, implemented in the software TreMuri [29], was subjected to static and dynamic nonlinear analyses. The application of pushover analyses was based on an incremental lateral force proportional to the first vibration mode, whereas the time history analyses involved real ground motion records properly scaled to match the response spectrum.

Erberik [30] assessed the seismic vulnerability of Turkish masonry buildings through the application of static and dynamic nonlinear analyses using the software SAM [31]. The buildings were classified into different groups considering criteria such as the number of stories, material, length of walls and openings and regularity in plan. Two shear capacity-based LSs and PGA as IM, which ranged between 0.01 g and 0.80 g, were established for the assessment of the seismic vulnerability of such structures. Additional investigation associated with masonry structures can be found in [32-34].

Most of the investigations conducted so far are based on simplified numerical models which do not allow to consider the interaction between in-plane and out-of-plane mechanisms. In addition, they mainly focused on the seismic response of URM structure due to the application of nonlinear static analysis, which neglects the degradation of stiffness and strength due to the unloading and reloading cycles. In this sense, the assessment of the seismic vulnerability of URM structures requires thorough methodologies based on the use of numerical strategies able to provide a more realistic earthquake response still maintaining a low computational burden. This paper aims at proposing a methodology for the seismic vulnerability assessment of an URM structure using a simplified computational tool capable of simulating the in-plane and out-of-plane mechanisms. The computational tool, named Discrete Macro-Element Modeling (DMEM) approach, is also characterized by a reduced number of degrees of freedom (DOFs) which allows the application of nonlinear dynamic analysis with a low computational demand. In addition, a multidirectional pushover analysis technique is used for the definition of the displacement capacity of the URM structure. Based on the results of this investigation, it was possible to demonstrate the applicability of this methodology for the assessment of the seismic vulnerability of URM structures.

2. The Discrete Macro-Element Modeling (DMEM) approach

An alternative modeling approach for assessing the in-plane response of masonry structures was initially introduced by Caliò, et al. [35] in which masonry structures were represented by means of two-dimensional panels. Each panel can be represented according to a mechanical scheme composed by a rigid hinged quadrilateral and two diagonal nonlinear links. As depicted in Figure 1a, the connection between two adjacent panels is ruled by a zero-thickness interface discretized with a number of nonlinear links placed in the direction orthogonal to its length and a single nonlinear link placed along its length.

This simplified modeling approach is capable of simulating the main in-plane failure mechanisms of masonry structures which are governed by a different set of nonlinear links. The flexural mechanism, associated with the crushing of masonry in the compressive area and the rupture in the tensile area, is governed by the nonlinear links orthogonally distributed along the length of the interface element. The in-plane shear-sliding mechanism or slipping of masonry in the direction parallel to the mortar joints, which occurs for low values of cohesion or friction force, is simulated by means of the single sliding nonlinear link in the interface element. Finally, the in-plane shear-diagonal mechanism, related to the formation of diagonal cracking, as a consequence of low values of tensile strength, is ruled by the couple of diagonal nonlinear links at the panel. The kinematics of each panel is described by four Lagrangian parameters associated with the rigid body motion and the shear deformability of a masonry panel.

The plane mechanical scheme can be efficiently adopted for describing the global response of masonry buildings governed by the in-plane behavior of masonry walls assuming that the out-of-plane mechanics are prevented. In order to overcome this significant restriction, an upgrade of the plane element was carried out by Pantò, et al. [36]. The extension of the element to spatial behavior has been obtained by introducing two-dimensional interface element characterized by new sets of nonlinear links allowing the simulation of out-of-plane mechanisms. The two-dimensional interface element is now discretized into a matrix of transversal nonlinear links which aim at governing the bi-flexural

mechanism of this type of structures. The out-of-plane sliding and the torsional responses of URM structures are simulated by two additional links which are placed along the thickness of the interface element. As illustrated in Figure 1b, the mechanical scheme of the upgraded model is now composed of four rigid plates connected by hinges and a single diagonal nonlinear link which governs the in-plane shear-diagonal mechanism of URM structures. The kinematics associated with a single spatial panel is described by seven kinematic variables associated with the rigid body motion and the in-plane shear deformability of the corresponding masonry panel.

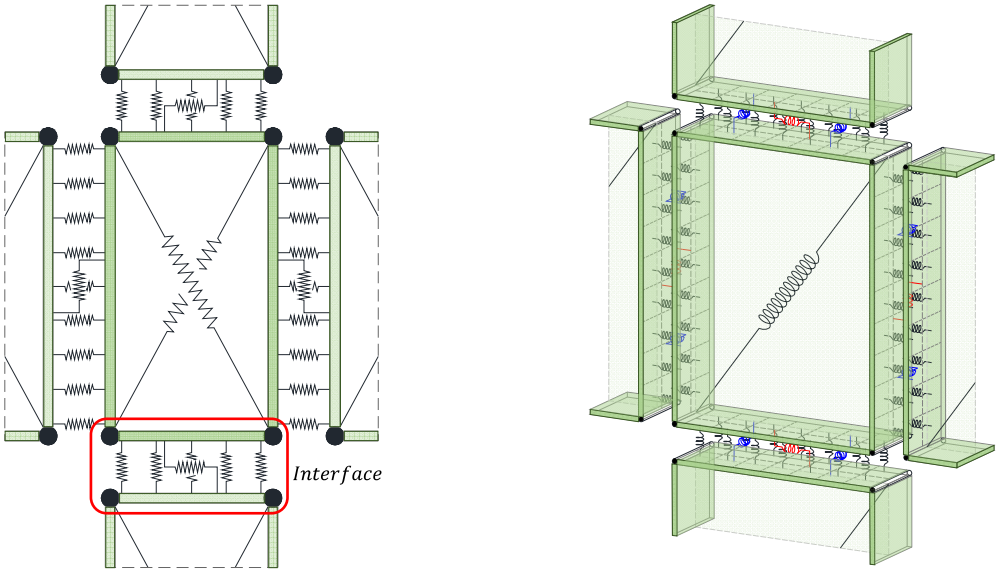

(a) (b)

Figure 1. Discrete Macro-Element Modeling approach: (a) two- and (b) three-dimensional mechanical configurations.

An accurate simulation of the combined interaction between in-plane and out-of-plane responses of URM structures requires adequate calibration procedures for each set of nonlinear links. Different methodologies are followed for estimating the linear mechanical properties of the links at an interface level and the diagonal link placed on each panel. The calibration procedure associated with the transversal and sliding links is based mainly on a fiber approach. Based on this approach, each adjacent panel is divided into a compound of fibers in accordance with the discretization of the connecting interface element. Each fiber represents a strip of masonry in a given direction, and it is characterized by an

influence area (A_F for the transversal links, and A_S for the sliding link), and an equivalent length l. In the case of rectangular elements, the initial flexural stiffness k_F, related to the transversal links, is reported in equation (1) where E represents the masonry Young's modulus. The initial stiffness k_S associated with the sliding response, expressed in equation (2), is defined as a function of the shear modulus G and a shear factor denoted as α_S whose value ranges between 0 and 1 [36]. This parameter describes the contribution of the in-plane sliding links and the diagonal link on the overall in-plane elastic shear stiffness of the DME model. If it presents a value equal to 1, the in-plane sliding links are characterized by a rigid behavior and the overall in-plane stiffness is given by the diagonal links. The out-of-plane links contemporary govern the out-of-plane shear and torsion stiffness of the masonry macro portion simulated by the DME model. The elastic stiffness of each link is evaluated according to an afference volume associated with half A_S (Figure 2c) while its mutual distance d, given in equation (4), is estimated in order to reproduce the elastic torsional stiffness of the masonry portion (k_ϕ). The latter is evaluated according to equation (3) where J_ϕ is the torsional rigidity factor of the panel cross section.

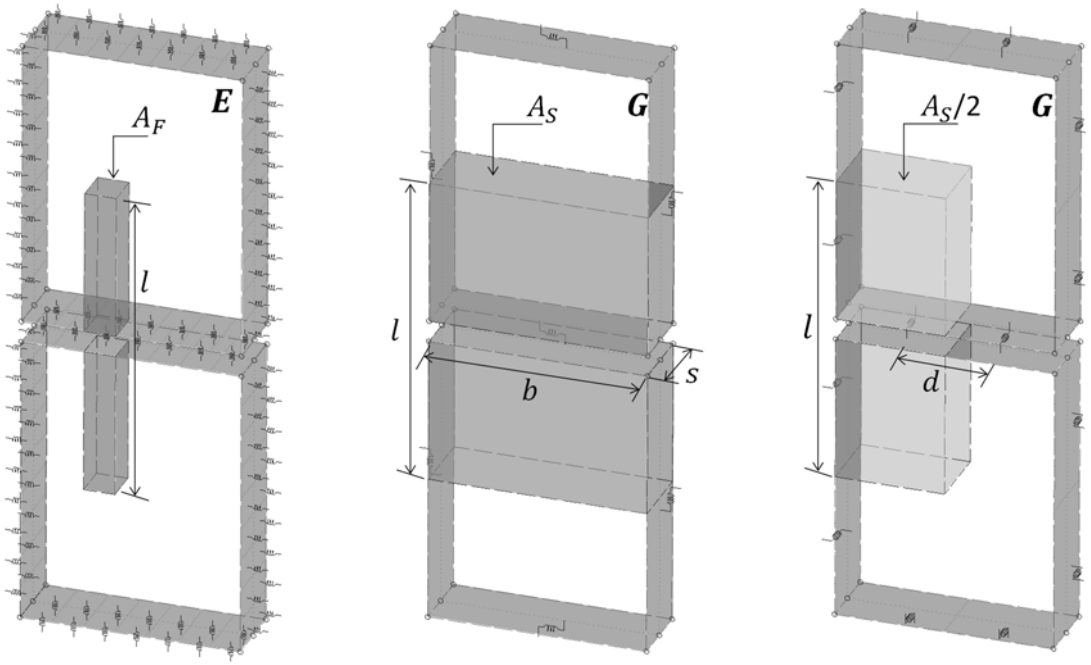

(a) (b) (c)

Figure 2. Fiber calibration procedure for: (a) transversal links, (b) in-plane and (c) out of plane sliding links.

$$k_F = \frac{2EA_F}{l} \tag{1}$$

$$k_s = \frac{GA_s}{l(1-\alpha_s)} \tag{2}$$

$$k_\phi = \frac{G}{l} J_\phi = \frac{G}{l}\left\{ bs^3 \left[\frac{1}{3} - 0,21\frac{s}{b}\left(1 - \frac{s^4}{12b^4} \right) \right] \right\} = \tag{3}$$

$$d = 2s\sqrt{\frac{1}{3} - 0,21\frac{s}{b}\left(1 - \frac{s^4}{12b^4} \right)} \tag{4}$$

The nonlinear and cyclic behaviors of these links (transversal and sliding) are characterized by different constitutive models. The nonlinear response of the transversal links is described by exponential (tension) and parabolic (compression) constitutive laws. The cyclic behavior of these links corresponds to a hysteretic Takeda model [37]. Due to the frictional phenomenon of the sliding links, their nonlinear behavior is described by a Mohr-Coulomb yielding criterion, whereas the cyclic response of this set of links is associated with an elasto-plastic hysteretic model. The cyclic constitutive models for these typologies of nonlinear links, namely the transversal and sliding links, are illustrated in Figure 4 in which F_t and F_c are the tensile and compression strengths of transversal links (Figure 2a), whereas F_y corresponds to the ultimate strength sliding links (Figure 2b).

The calibration procedure of the diagonal nonlinear link is conducted by enforcing an equivalence between a finite portion of masonry with pure shear deformability, as shown in Figure 3. Based on this equivalence, the shear diagonal stiffness k_D is given as a function of the shear modulus G, the transversal area A_T, the shear factor α_s, the height h, and the angle $\omega = arctan\ (h/b)$ described between the diagonal link and the horizontal edge of the panel. The expression that describes the initial shear-diagonal stiffness is reported in equation (5).

$$k_D = \frac{GA_T}{\alpha_s h \cos^2 \omega} \tag{5}$$

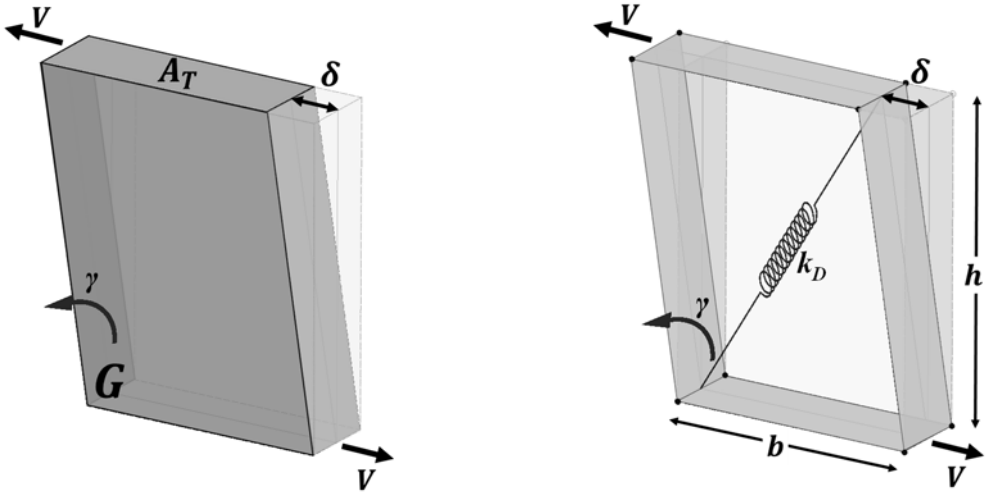

(a) (b)

Figure 3. Calibration of diagonal link: (a) finite portion of masonry subjected to pure shear deformation, and (b) rectangular panel.

Two different yielding criteria can be established for the description of the post-elastic behavior of the diagonal links. These criteria, named Mohr-Coulomb and Turnsek and Cacovic [38], take into consideration the confinement condition to which masonry is subjected for the definition of the shear capacity. The diagonal nonlinear links are also characterized by a cyclic response governed by a Takeda hysteretic model [37] in which the unloading cycles recover the initial stiffness. The cyclic constitutive model for the nonlinear diagonal link is illustrated in Figure 4c in which F_v corresponds to its ultimate strength. Further details regarding the calibration procedure and the cyclic behavior of these sets of links are reported in [39]. The proposed modeling approach has been implemented in the structural code HiStrA (Historical Structure Analysis) software [40].

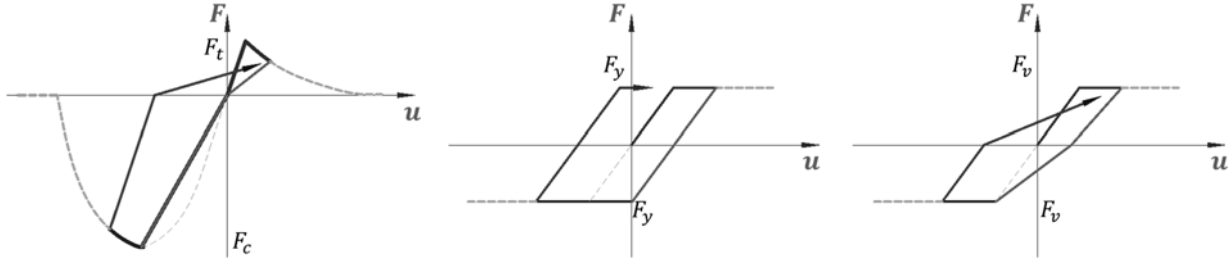

(a) (b) (c)

Figure 4. Constitutive models and hysteretic behavior of the different typologies of nonlinear links: (a) transversal, (b) sliding, and (c) diagonal.

3. Proposed procedure for seismic vulnerability assessment

Seismic vulnerability assessment is often conducted by means of analytical fragility functions which are capable of providing the probability of a structure to reach or exceed a LS due to a given IM. A fragility curve can be described by a normal cumulative distribution function Φ, which is characterized by a mean value θ and a standard deviation β as reported in equation (6). In most investigations associated with masonry structures, the derivation of fragility curves usually involves the application of nonlinear static analyses using simplified numerical tools aiming at reducing the computational demand. Several of these formulations are based on overly simplified numerical models neglecting some relevant aspects of URM structures such as the occurrence of out-of-plane mechanisms. Aiming at obtaining more realistic results, this investigation proposes a different methodology for the assessment of URM buildings which involves the use of nonlinear static and dynamic analyses performed by means of the discrete macro-element method previously introduced.

$$P(LS \mid IM = x) = \Phi\left(\frac{\ln(x/\theta)}{\beta}\right) \tag{6}$$

The procedure for the seismic vulnerability assessment of URM structures presented in this paper involves three main activities: i) definition of seismic input, ii) definition of adequate LSs and their corresponding capacity, and iii) derivation and fitting of the fragility curves. Since the proposed modeling approach is characterized by a reduced number of DOFs, and therefore a low computational demand, the seismic vulnerability assessment is performed by nonlinear static and dynamic analyses. In this sense, it is necessary to define proper seismic accelerograms, consistent with the design spectra, which can be associated with real ground motion records as well as synthetic or artificial accelerograms (first activity). Here, accelerograms artificially generated, following specifications reported in standards, have been adopted.

For the definition of accurate capacities for the selected LSs (second activity), a novel approach, based on multidirectional pushover analyses, is

proposed. This approach involves the application of a set of nonlinear static analyses, along different directions, with an incremental angular step as reported by Cannizzaro, et al. [41]. The result, denoted as *Capacity Dominium* (CD), allows the definition the displacement capacity as a function of the direction of the input for each defined LS. It is worth to note that, based on this alternative approach, different displacement-based criteria can be used for the definition of the LSs.

The derivation of the fragility curves (third activity), implies the introduction of uncertainty in the numerical model. In this investigation, the uncertainty is associated with the seismic input (scaled artificial accelerograms) and with other parameters such as mechanical properties or geometric configurations. This last activity also involved a fitting procedure for the estimation of the true probability, which considers the total number of analyses and the ones that led to the exceedance of the LS. As reported by Baker [42], a fitting process is given by a maximum likelihood approach aiming at optimizing the mean value θ and standard deviation β that characterize the fragility function. The true probability P of exceeding a LS due to the j^{th} IM is given by the binomial distribution p reported in equation (7) in which z and n correspond, respectively, to the total and exceeding number of nonlinear dynamic analyses, denoted as events hereafter. The likelihood function can be computed as the product of the binomial distributions associated with the different m levels of IMs, as reported in equation (8). The fitting procedure consisted of estimating the optimum values of θ and β, which provide the maximum likelihood.

$$P(z_j \text{ collapse in } n_j \text{ events}) = \binom{n_j}{z_j} p_j^{\,z_j} \left(1 - p_j\right)^{n_j - z_j} \tag{7}$$

$$Likelihood = \prod_{j=1}^{m} \binom{n_j}{z_j} \Phi\left(\frac{\ln\left(x_j/\theta\right)}{\beta}\right)^{z} \left(1 - \Phi\left(\frac{\ln\left(x_j/\theta\right)}{\beta}\right)\right)^{n-z} \tag{8}$$

The proposed methodology presents two novel contributions, namely, the application of multidirectional pushover analysis for the definition of the displacement capacity, and the application of extensive nonlinear dynamic analyses for the derivation of fragility curves when considering more detailed numerical models capable of considering the interaction between in-plane and out-

of-plane mechanisms. Firstly, the CD allows a proper identification of LSs since it can be combined with different LSs criteria, and it can also be applied to any structural typology. Secondly, time history analysis constitutes a more precise tool for the assessment of the seismic response of structures since it involves energy dissipation as well as the degradation of strength and stiffness of the material.

4. Application to a brick masonry structure

The proposed procedure for the seismic vulnerability assessment of URM structures was applied to a brick specimen characterized by a strong out-of-plane collapse mechanism. The seismic response of such masonry structure was thoroughly investigated by means of shaking table tests [43] as well as numerical simulations [39] according to a deterministic approach. The case study and the main results previously obtained are here briefly recalled. As depicted in Figure 5a, the considered U-shape structure was composed of three walls: a main gable and two return walls with an equal thickness of 0.235 m. The base of the main gable wall was equal to 3.50 m whereas its height presented a value of 2.75 m at the top of the tympanum. The base and height of both return walls were equal to 2.25 m and 2.50 m, respectively. This URM structure also presented two window openings: one at the main gable wall and another one at one return wall with dimensions of 0.80 x 0.80 m^2 and 0.80 x 1.00 m^2, respectively. The unusual geometry of the prototype, characterized by a U-shape plan layout, was chosen with the aim to investigate the behavior of the main gable wall taking into account the possible constraining effect of typical return walls. In the experimental campaign. the brick masonry structure was subjected to the 2011 Christchurch earthquake which was applied in the direction perpendicular to the main gable wall (Y-direction in Figure 5a). The out-of-plane behavior of the structure was also investigated by means of two numerical approaches, namely FE and Discrete Macro-Element (DME) models characterized by a different discretization, as illustrated in Figure 5b and Figure 5c respectively. The FE model was built using the DIANA software [44], and it was characterized by a rotation total strain crack model. The element type used for the FE model consisted of twenty-node bricks CHX60 which were described by a 3x3x3 integration scheme [44]. On the other

hand, the DME model was implemented by means of the HiStrA software [40], using the constitutive laws for the nonlinear links presented in Section 2. These numerical models presented a great difference in terms of DOFs: 54477 for the FE model, and 616 for the DME model. Both models were subjected to static and dynamic nonlinear analyses for investigating the out-of-plane response of the main gable wall. Mass proportional pushover analyses and nonlinear dynamic, consistent with the seismic input recorded during the shaking table tests (see Figure 5f), have been applied in the direction perpendicular to the main gable wall (Y-direction in Figure 5b-c). Figure 5d shows the significant agreement between the two modeling approaches when performing pushover analyses, especially in the negative direction (-Y). It can be noted that there is a good agreement in maximum capacity in the +Y-direction, but the residual forces of these two modelling approaches are somehow different due to their corresponding failure mechanisms. In the case of the FE model, the collapse is governed by in-plane and out-of-plane mechanisms, whereas, in the case of the DME model, the response is centered on the main gable wall. The comparison in terms of time history analyses is depicted in Figure 5e demonstrating the capability of the proposed modeling approach of providing a satisfactory simulation of the dynamic response of a sophisticated model with a strongly reduced computational burden (96%). The duration of the nonlinear dynamic analysis associated with a FE model was approximately [39],Figure 5g[39].

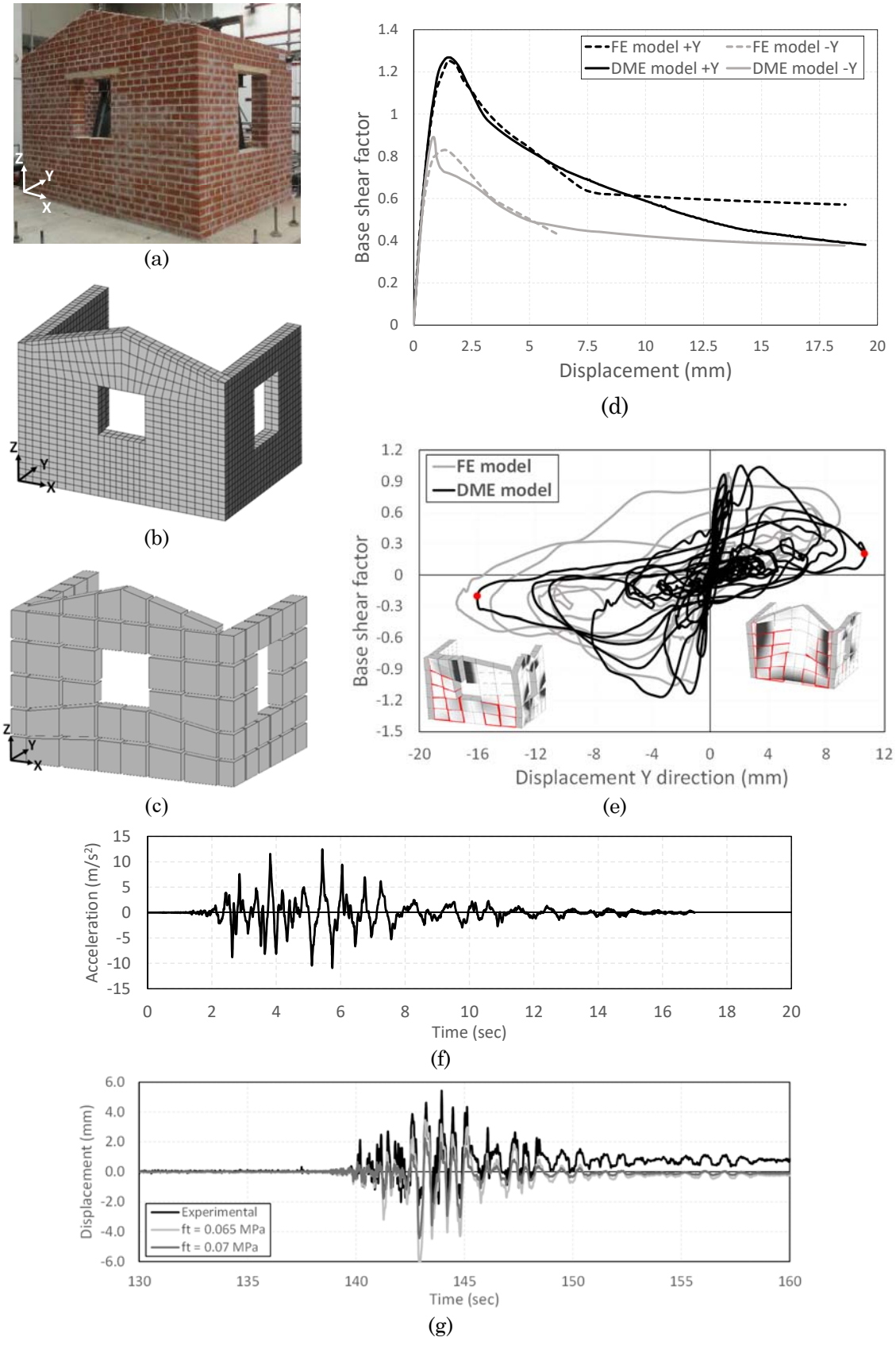

Figure 5. Brick masonry structure: (a) benchmark, (b) FE, (c) DME model, and comparison in terms of (d) pushover, (e) time history analyses , and (f) seismic input, and (g) experimental and numerical history of displacement [39].

4.1. *Step 1: Definition of seismic input*

Aiming at assessing the seismic vulnerability of the considered brick masonry structure, nonlinear dynamic analyses, performed on the DME model, have been based on uniaxial as well as three-component artificial accelerograms. The uniaxial seismic inputs have been applied in the direction perpendicular to the main gable wall in order to investigate its out-of-plane response when the excitation acts in the orthogonal direction only. The three-component artificial accelerograms have been applied to the structure to investigate the response of the gable walls under in-plane, out-of-plane and vertical base acceleration components. The artificial accelerograms were generated so that they match the horizontal and vertical elastic response spectra with 5% of viscous damping as specified by the EC8-Part1 [45]. Type 1 and Type 2 elastic response spectra, respectively associated with far- and near-field seismic inputs, were taken into consideration for this investigation. The horizontal S_{he}(T) and vertical S_{ve}(T) components of these spectra are illustrated in Figure 6, and their definition is given in [45].

The generation of the artificial accelerograms was conducted considering a reference horizontal design ground acceleration a_g equal to 1 g and 5% of viscous damping ($\eta = 1$). Assuming that the brick masonry structure was located in a Lisbon area, the soil factor S was established as 1, which corresponds to a class A soil (rigid soil). The reference spectrum periods T_B, T_C and T_D were established considering the Portuguese National Annex [46]. This code also provides a ratio between vertical (a_{vg}) and horizontal (a_g) design ground accelerations. The different parameters required for the definition of the elastic response spectra Type 1 (far-field earthquakes) and Type 2 (near-field earthquakes) are summarized in Table 1.

Table 1. Parameters for the definition of horizontal elastic response spectrum.

Component	Elastic response spectrum	Soil type	S	a_{vg}	H	T_B (s)	T_C (s)	T_D (s)
Horizontal	Type 1	A	1	-	1	0.10	0.60	2.00
	Type 2	A	1	-	1	0.10	0.25	2.00
Vertical	Type 1	-	-	0.75 a_g	1	0.05	0.25	1.00
	Type 2	-	-	0.95 a_g	1	0.05	0.15	1.00

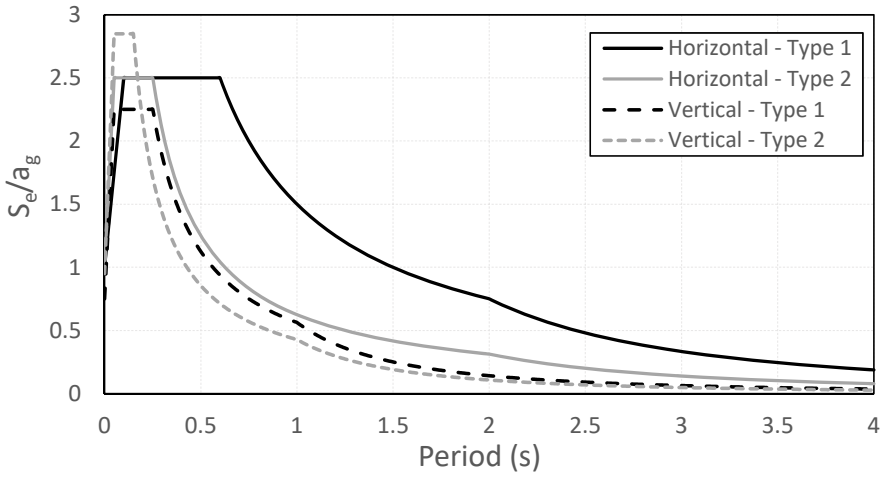

Figure 6. Elastic response spectra used for the generation of artificial accelerograms.

In addition to the elastic response spectra, the generation of artificial seismic input also required the definition of minimum duration of stationary part of acceleration. In accordance with the Portuguese National Annex [46], far- and near-field based artificial accelerograms are characterized by stationary times of 30 seconds and 10 seconds, respectively. In this sense, the artificial accelerograms were generated considering total durations of 40 seconds for far-field earthquakes and 20 seconds for near-field earthquakes. The generation of artificial accelerograms was conducted using the software SIMQKE [47]. An initial set of 1200 horizontal and 600 vertical samples were generated between Type 1 and Type 2 earthquakes. Since both horizontal components need to be uncorrelated, their generation was conducted separately. The accuracy of this initial set was assessed by the comparison between the spectrum of each accelerogram and the elastic response spectrum used for its generation. The artificial accelerograms whose spectrum lacked resemblance with its corresponding elastic response spectrum were discarded from the initial set. The selection of suitable samples led to a final set of 560 horizontal and 280 vertical artificial accelerograms which were subsequently subjected to a baseline correction by means of the software LNEC-SPA [48]. A high pass Fourier filter of 0.20 Hz and a cosine-based windowing approach were considered for the signal processing of the accelerograms.

4.2. Step 2: Definition of displacement capacity

The definition of appropriate limit states LSs constitutes a relevant task for seismic vulnerability assessment. The LSs can be evaluated considering the capacity of a structure in terms of interstory drift, damaged area, hysteretic energy or base-shear resistance. From the different approaches, the assessment of the seismic vulnerability of masonry structures is usually conducted based on interstory drift procedures. For instance, the EC8-Part3 [9] establishes three LSs, namely Damage Limitation, Significant Damage and Near Collapse, together with their corresponding displacement capacity. The capacity associated with the first LS is given by the yielding displacement, whereas the definition of the capacity related to the second LS depends on the type of failure mechanism, namely flexural and shear. The capacity of the remaining LS (Near Collapse) is defined as 4/3 of the drift associated with a Significant Damage LS. Nevertheless, the definition of these interstory drift capacities is related to masonry structures with a box-type behavior; and therefore, they are not suitable for structures with predominant out-of-plane collapse mechanisms. The multiscale approach proposed in [17, 18] may be considered as a proper formulation for the definition of LSs of the masonry structure under investigation; however, due to its predominant out-of-plane behavior as well as its irregular geometrical characteristics, it was decided to adopt an alternative procedure. In this regard, the CD constitutes a tool that enables the evaluation of the global response of the structure allowing a comprehensive representation of the capacity of the building and a proper identification of LSs.

The EC8-Part3 [9] and the Italian Code [11] relate the definition of LSs to the base shear of the structure. These LSs, namely Near Collapse for the former and Life Safety for the latter, are established when a structure experiences a 20% loss of its maximum shear resistance (ultimate displacement). For the proposed methodology, such shear capacity based formulation was taken into consideration for the definition of two of the LSs, namely Near Collapse and Significant Damage. The definition of the first LS (Damage Limitation) was given by the yielding displacement as specified in the EC8-Part 3 [9]. A summary of the LSs used in this

498 investigation, together with their corresponding displacement capacity, is
499 reported in Table 2.

Table 2. Limit states and displacement capacity for the assessment of the seismic vulnerability of the brick masonry structure.

Limit State	Capacity definition
Damage Limitation	u_y (yielding displacement)
Significant Damage	$3(u_u)/4$
Near Collapse	u_u (ultimate displacement at 20% reduction of capacity)

500 In the proposed methodology, the definition of the displacement capacity
501 of the LSs involves the application of an alternative procedure denoted as *Capacity*
502 *Dominium* (CD) [49]. In this procedure, the structure is subjected to a set of
503 nonlinear static analyses along different angles aiming at assessing its global
504 response. For this investigation, the brick masonry structure was subjected to a
505 set of sixteen analyses with an incremental angular step of 22.5º as illustrated in
506 Figure 7. These analyses were performed by applying an incremental force
507 proportional to the mass in each direction. The mechanical properties of the DME
508 model were adopted according to [39] which are reported as the mean values in
509 Table 3. The global response of the structure was evaluated by considering the
510 control nodes with highest out-of-plane displacements: one located at the top of
511 the tympanum and two placed at the top of the end of both return walls.

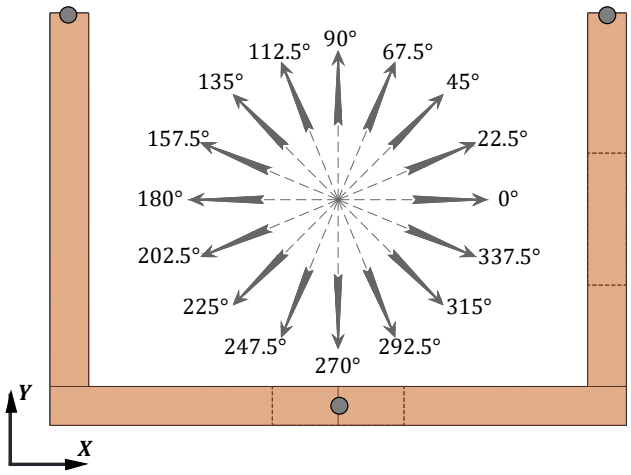

Figure 7. Application of nonlinear static analyses for the definition of the LSs based on a Capacity Dominium procedure.

The CD for a Near Collapse LS was built taking into consideration the sixteen pushover curves until a 20% loss of maximum shear capacity was attained. As illustrated in Figure 8a, the pushover curves were plotted backward, along their corresponding angles, and at an equal distance of 8 mm from the origin **O**. Subsequently, patches were employed to connect each pushover curves aiming at the definition of a color map basket domain (see Figure 8b) which corresponds to a three-dimensional representation of the global capacity of the brick masonry prototype. In Figure 8, the vertical axis is associated with the load factor (ratio between base shear and self-weight), whereas the horizontal axes are related to the horizontal displacements in X and Y directions, respectively.

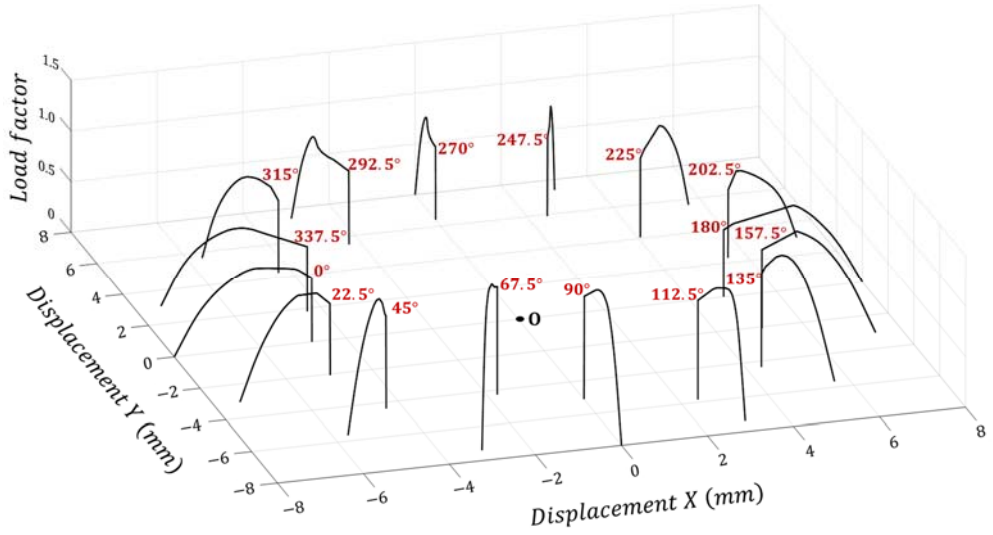

(a)

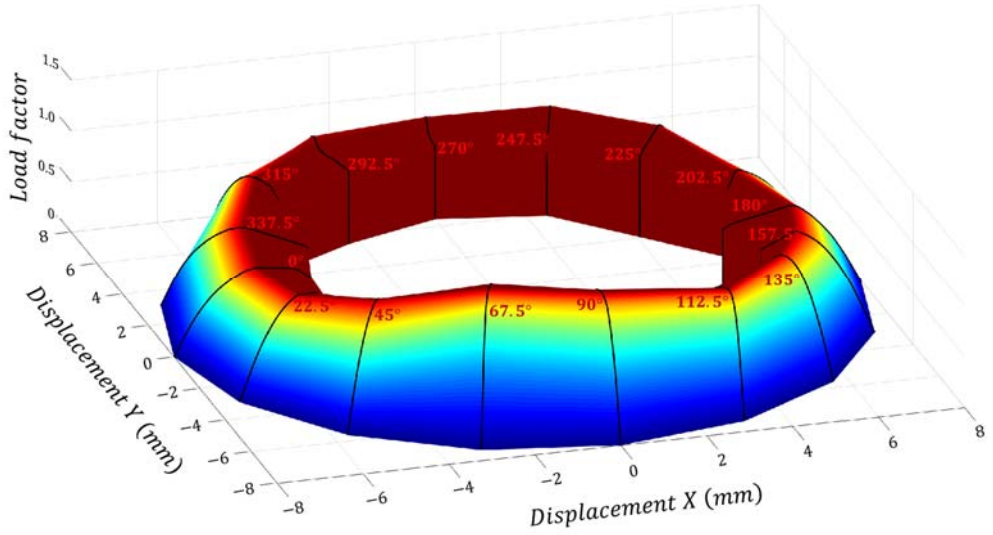

(b)

Figure 8. Construction of basket domain based on the application of pushover analyses along different angles.

The CD associated with the Near Collapse LS can be determined as the effective displacement field in the three-dimensional basket domain as shown in the gray area in Figure 9a. Such displacement field is created by connecting a set of nodes in accordance with the different pushover curves and their corresponding angle plotted in the three-dimensional basket domain. These contouring nodes are located at a distance d_a equal to the ultimate horizontal displacement from the origin O. Following a similar approach and considering the specifications provided by the EC8-Part3 [9], the CD for the two additional LSs were also properly established. In the case of the Damage Limitation LS, the displacement field was associated with the yielding displacement and it is given by the blue area in Figure 9b. The CD for a Significant Damage LS was defined as a ratio of 3/4 with respect to the Near Collapse LS (red area in Figure 9b) as stated by the EC8-Part3 [9]. It is remarkable how the CDs change shape as a function of the LS. As an example, the +X/–Y sector is rather stringent in terms of Damage Limitation LS, while the –X/–Y sector becomes rather stringent for the Significant Damage and Near Collapse LSs, when compared with the remaining LSs in the same sector. This behavior can be associated with the presence of a window opening in one return wall which introduces asymmetry to the structure. In addition, it is possible to notice that different shapes of the CDs in the –Y and +Y sectors. These different shapes are given by the asymmetry generated by the window openings but also by the influence of the return walls on the global stiffnesses of the structure and their capacity to deform.

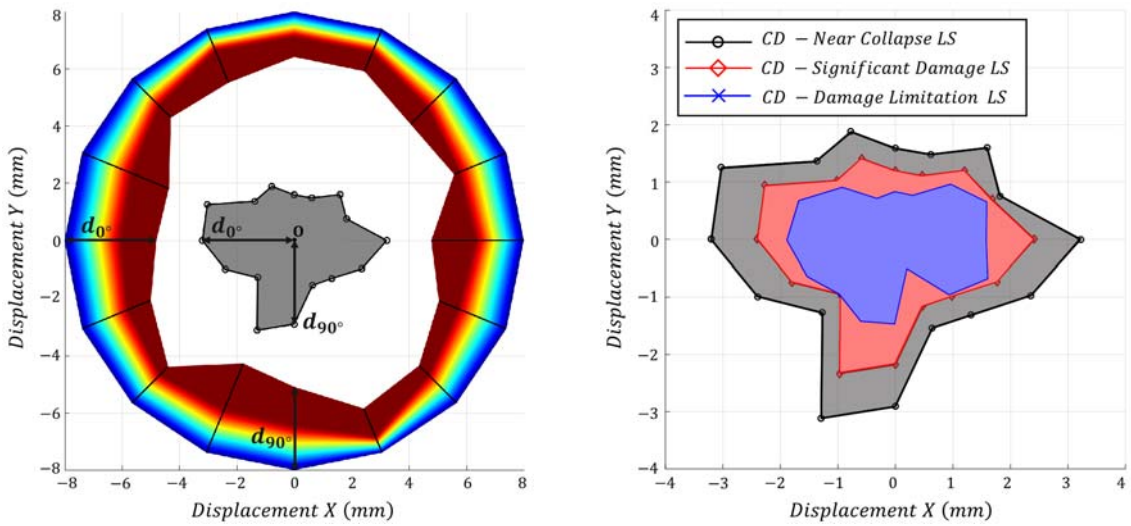

(a) (b)

Figure 9. Displacement capacity: (a) creation of effective displacement field, and (b) Capacity Dominium for the selected LSs.

4.3. *Step 3: Derivation and fitting of analytical fragility curves*

In this work, the seismic vulnerability of the masonry structure was assessed by the derivation of analytical fragility curves through the application of nonlinear dynamic analyses. For this purpose, the DME model of this prototype was subjected to artificial accelerograms compatible with the design spectra. Although the generation of the seismic input constitutes a significant source of uncertainty, it is necessary to consider different sources of uncertainty in order to conduct a more reliable seismic vulnerability assessment. These additional uncertainties have been mainly focused on mechanical properties which require the definition of probability density functions (PDFs) together with mean values and coefficients of variation (COVs). The mean values and COVs of material properties such as Young's modulus E, specific weight γ, compressive f_c, and tensile f_t strength, were established based on the mechanical characterization conducted by Candeias, et al. [43]. In such investigation, simple and diagonal compression tests were conducted to the brick masonry in order to determine the latter mechanical properties as well as their statistical characteristics. The mean values of other mechanical properties, namely, tensile fracture energy G_f^I, shear modulus G, shear strength f_{y0}, cohesion c, and friction coefficients associated with the diagonal and sliding failure modes (μ_d and μ_s), were defined as the parameters presented in the seismic assessment of the brick masonry structure conducted in

564 [39]. On the other hand, the mean values of the fracture energies in compression
565 G_c and shear-sliding G_f^{II}, were given as a function of ductility indexes as reported
566 in literature. For instance, Lourenço [50] provided average values for ductility
567 indexes in compression d_{uc} and shear-sliding d_{us} equal to 1.6 mm and 0.09 mm,
568 respectively. The definition of COVs for the mechanical properties associated with
569 the shear mechanisms (diagonal and sliding) followed the specifications provided
570 by the JCSS Probability Model Code [51]. In the case of shear strength and
571 cohesion, the COV presented a value of 40%, whereas, in the case of friction
572 coefficients, this value was equal to 19%. Due to the lack of information related to
573 the remaining mechanical properties, it was assumed that their corresponding
574 COVs corresponded to 30%. The statistical characteristics for the mechanical
575 properties are summarized in Table 3. In this investigation, the uncertainty was
576 also focused on other geometrical and structural parameters such as thickness and
577 viscous damping ratio. In the case of the wall thickness, a mean value of 23.5 cm
578 and a COV of 5% were established as statistical characteristics. The viscous
579 damping ratio presented a mean value of 3%, and due to the lack of information
580 associated with this structural parameter for URM structures, it was assumed
581 that it presented a COV of 30%. It is worth to note that the different uncertain
582 parameters (mechanical, geometrical and structural) were characterized by a
583 lognormal PDF.

Table 3. Probabilistic models associated with the mechanical properties of the DME model.

Parameter				Mean	Coefficient of Variation
Elastic behavior	Young's modulus	E	N/mm^2	5170	29%
	Shear modulus	G	N/mm^2	2133	30%
	Specific weight	Γ	N/mm^3	18.9x10^{-6}	3%
Tensile behavior	Tensile strength	f_t	N/mm^2	0.1	19%
	Fracture energy	G_f^I	N/mm	0.012	30%
Compressive behavior	Compressive strength	fc	N/mm^2	2.48	14%
	Compressive ductility index	d_{uc}	mm	1.6	30%
Shear-sliding behavior	Cohesion	c	N/mm^2	0.1	40%
	Friction coefficient	μ_s	-	0.7	19%
	Shear-sliding ductility index	d_{us}	mm	0.09	30%
	Shear strength	f_{y0}	N/mm^2	0.07	40%

Shear-diagonal behavior	Friction coefficient	μ_d	-	0.6	19%

The seismic vulnerability of the brick masonry structure was initially evaluated through the application of a set of 2000 time-history analyses based on uniaxial artificial accelerograms (along the Y direction, perpendicular to the main gable wall). From this initial set, 1000 analyses were associated with far-field seismic input (Type 1), whereas the remaining 1000 were related to near-field seismic input (Type 2). Each of these sets was subsequently divided into eight groups of 125 analyses in order to consider different intensity levels of PGA. Since the artificial accelerograms were generated with a horizontal design acceleration equal to 1 g, it was necessary to scale them aiming at comprising a wide range of PGA. In this case, eight scaling factors ranging between 0.45 and 0.80 (with an incremental step of 0.05) were defined for the seismic vulnerability assessment of the brick masonry structure. In order to define the uniaxial seismic inputs, 125 horizontal components were randomly selected from the corresponding final set of artificial accelerograms generated in Section 4.1. Subsequently, 125 random values of the different uncertain geometrical and mechanical parameters were defined based on their corresponding mean value, COV, and PDF. It is worth noting that the computational demand required for the assessment of the seismic vulnerability assessment of this structure was acceptable since the average duration of a single analysis was about 30 minutes using a conventional desktop.

An automatic routine was implemented for the application of time history analyses considering the variability of seismic inputs and uncertain parameters. The structural damping was assigned based on a Rayleigh criterion by considering natural frequencies of 18.8 Hz and 75.4 Hz as reported in [39]. These values were obtained after an eigenvalue analysis considering the mean values of the initial mechanical properties, and they remained constant despite the variation of properties such as the Young's modulus since it would require additional computational burden for the estimation of the dynamic properties for each time history analysis. Moreover, it is worth noticing that the contribution of viscous damping can be considered negligible if compared to the hysteretic dissipation considering the high non-linearity characterizing the structural response. The

614 definition of the mass properties of the numerical model was based on an efficient
615 diagonal mass matrix as reported in [52].
616 The CD related to each LSs, introduced in the previous sub-section, has
617 been obtained by analyzing the nonlinear response of the prototype when
618 subjected to static loading. The identification of the exceedance of a certain LS
619 when the structure is subjected to dynamic loading is not straightforward since
620 the displacement capacity of a structure subjected to earthquake dynamic loading
621 is generally higher, when compared to the corresponding capacity obtained for a
622 monotonic application of horizontal static loads. For this reason, it is necessary to
623 establish a conventional criterion for the exceedance of each LS. In the application
624 here performed in order to conduct the maximum likelihood fitting process, it has
625 been assumed that an exceeding event is given when the history of the horizontal
626 top displacements exceeds the area of its corresponding CD at least twice (a single
627 event is disregarded, while a second event is assumed as a confirmation. Initially,
628 the seismic vulnerability assessment was carried out considering that an event
629 exceeded a given LS when the dynamic response surpassed the CD at least once.
630 However, a single time could be considered as an impact or outlier caused by the
631 seismic input and not as the real collapse of the structure. Therefore, the events
632 in which the dynamic response remained inside the CD or surpassed only once the
633 displacement field were not included in the fitting procedure.
634 The assessment of the dynamic response due to the application of Type 2
635 uniaxial seismic input is illustrated throughout Figure 10 for the three LSs
636 defined for this investigation. In this figure, the responses associated with each of
637 the three control nodes selected for the definition of the CD were plotted together.
638 As it was expected, the dynamic response of the numerical model was strongly
639 characterized by histories of displacements in the Y direction (node at the top of
640 the main gable wall), since the seismic input was applied only in that direction.
641 The response of the other two control nodes did not present a significant
642 displacement since the dynamic load was applied in one direction. The assessment
643 was focused on the out-of-plane behavior of the façade; therefore, only the results
644 associated with the top of the tympanum as control node were considered for the

assessment of the seismic vulnerability of this structure. The number of exceeding events out of the 125 set of accelerograms are summarized in Table 4.

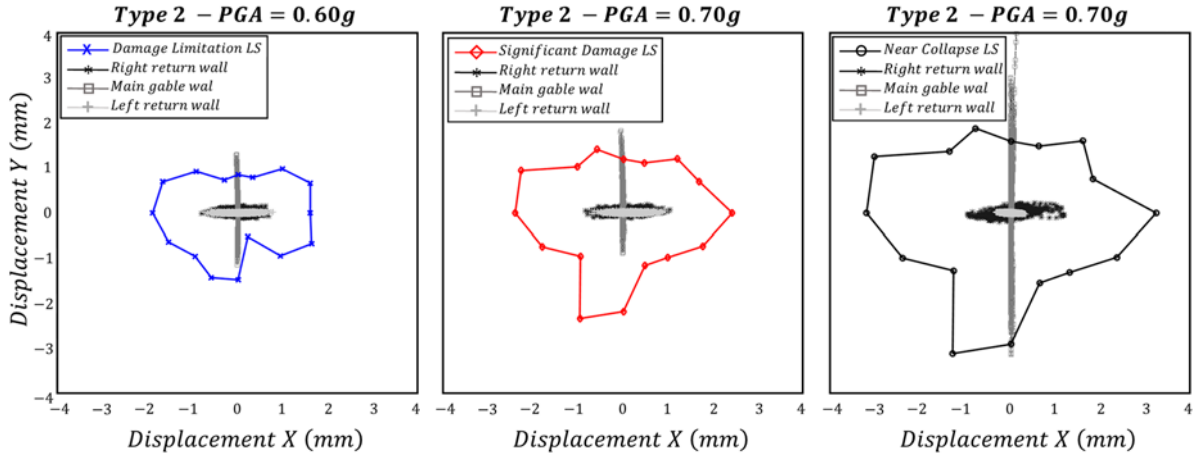

(a) (b) (c)

Figure 10. Assessment of seismic performance based on a Capacity Dominium due to the application of uniaxial artificial accelerograms to different LSs: (a) Damage Limitation , (b) Significant Damage, and (c) Near Collapse.

Table 4. Exceeding events for the derivation of analytical fragility curves due to the application of uniaxial artificial accelerograms (out of a set of 125).

IM	Number of events	Number of exceeding events					
		Damage Limitation LS		Significant Damage LS		Near Collapse LS	
		Type 1	Type 2	Type 1	Type 2	Type 1	Type 2
0.45 g	125	32	27	19	26	13	6
0.50 g	125	51	35	28	55	26	14
0.55 g	125	81	50	37	79	48	24
0.60 g	125	96	74	57	89	62	42
0.65 g	125	106	92	73	106	79	59
0.70 g	125	116	102	92	110	92	72
0.75 g	125	122	110	99	116	108	91
0.80 g	125	123	115	110	120	112	99

The fitted analytical fragility curves obtained from the application of uniaxial artificial accelerograms are illustrated in Figure 11. From these results, it is possible to determine the probability of exceedance of a LS due to the occurrence of a seismic event with a given value of PGA. In the case of far-field earthquakes, there is a 44% of probability of exceeding the Damage Limitation LS when the brick masonry structure is subjected to a seismic intensity of 0.50 g (see solid lines in Figure 11). This probability reduces to 31% and 22% when considering the Significant Damage and Near Collapse LSs, respectively. In a similar way, it is also possible to estimate the expected seismic intensity in terms of PGA for a desired probability of exceedance. For instance, the Damage

Limitation LS is exceeded with a probability of 50% when the PGA of the seismic input corresponds to approximately 0.52 g. In the case of the remaining LSs, the expected intensity of the uniaxial seismic input increases to 0.57 g and 0.61 g. It was also observed that the analytical fragility curves of the different LSs obtained from the application of uniaxial far-field seismic inputs were not so separated. Such behavior is strictly related to the characteristics of the CD and the definition of the capacity of the LSs since the displacement fields were close to each other as a result of the rapid loss of shear resistance and the quasi-brittle behavior of the material, as a consequence of the low-ductility capacity of the structure. The dashed lines in Figure 11 illustrate the analytical fragility curves associated with the application of near-field seismic input. In this case, the probabilities of exceedance of the different LSs were also estimated considering a seismic intensity of 0.50 g. For a Damage limitation LS, this probability corresponds to 42% which is slightly lower when comparing it to the one obtained with far-field seismic inputs. A stronger reduction was observed for the Significant Damage and Near Collapse LSs. In the former, the probability of exceedance presents a value of 22%, whereas, in the latter, such probability corresponds to 11%. In these cases, the reduction between far- and near-field probabilities is around 10%, and it may also be related to the characteristics of the seismic input such as frequency content and stationary time.

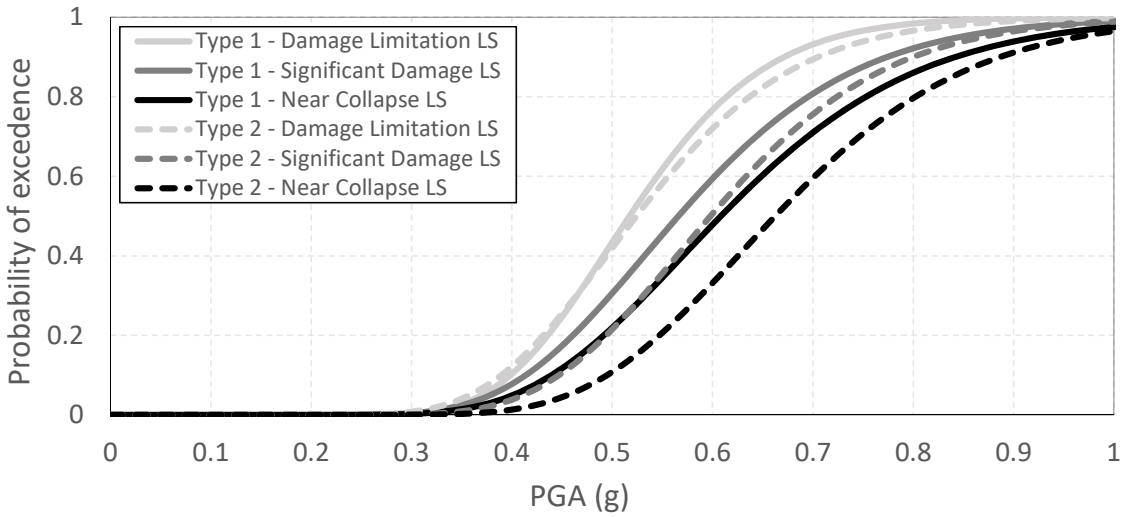

Figure 11. Analytical fragility curves derived due to the application of uniaxial artificial accelerograms.

A sensitivity analysis was conducted regarding the role that plays the times that the dynamic response surpasses the CD on the total number of exceeding events. As illustrated in Figure 12a, it can be stated that, when considered Type 1 seismic inputs, the analytical fragility curves do not present significant changes if three or four events are considered. On the contrary, the number of times that the dynamic response is outside the displacement capacity plays a slight influence when applying artificial accelerograms based on a Type 2 earthquakes (see Figure 12b). In the case of an IM equal to 0.60 g, the probability of exceeding a Damage Limitation LS presented a reduction of 6.4% when considering that the dynamic response is out of the CD at least four times. A similar behavior was noticed in the case of the remaining two LSs: reductions of 5.5% and 5.7% for a Significant Damage and Near Collapse LSs, respectively. It is worth noting that these may be considered as small reduction. Nevertheless, further investigations regarding the optimum number of times that the dynamic response should be outside the displacement capacity need to be conducted. In addition, different criteria can also be used for considering the overcapacity of the structure when subjected to dynamic loadings. The stabilizing effect of the inertial force distributions could be considered by accounting for a dynamic amplification factor of the static dominium. This additional alternative approach also requires further experimental data and will be the subject of future investigations.

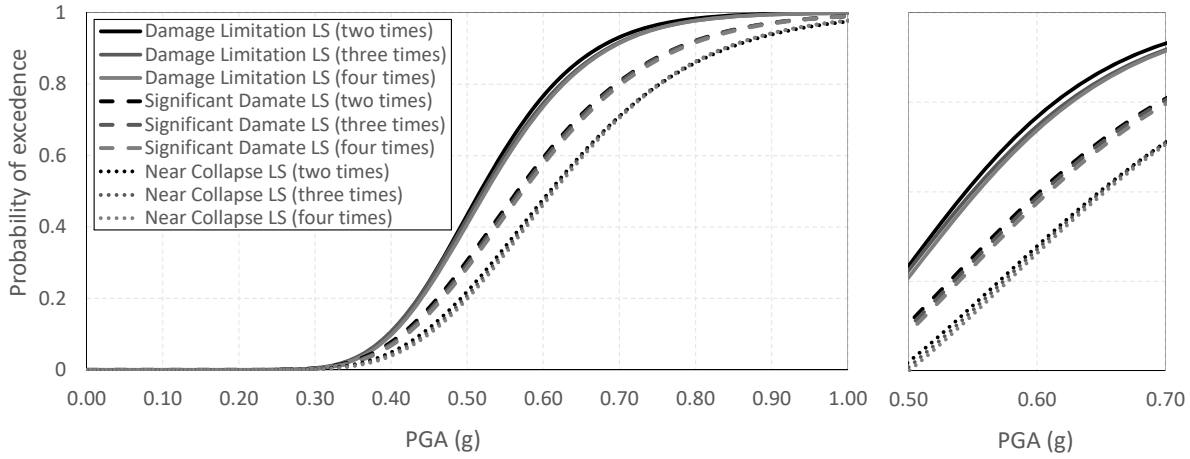

(a)

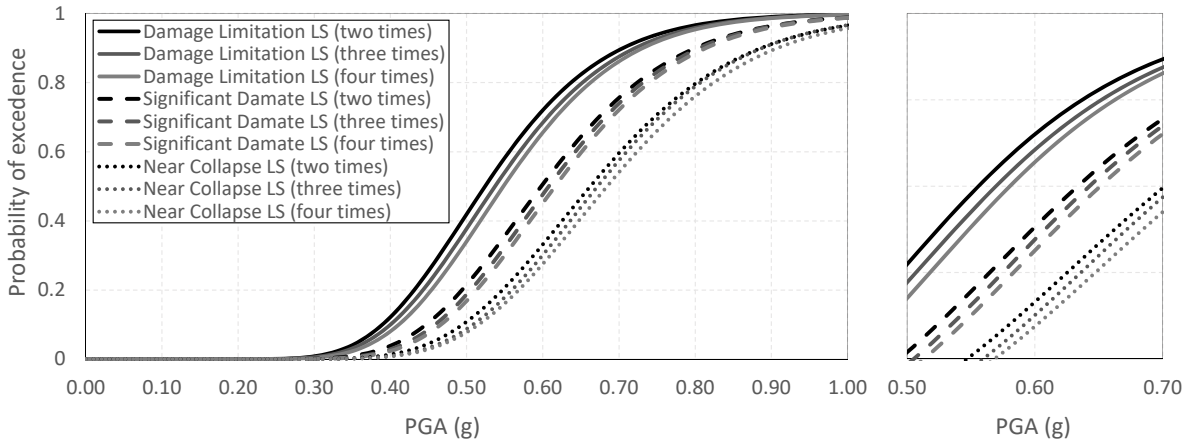

(b)

Figure 12. Sensitivity analysis regarding the number of times that dynamic response was outside the displacement capacity: (a) Type 1 and (b) Type 2 seismic inputs.

Following the same approach, the seismic vulnerability of the brick masonry structure was also assessed considering the influence of additional components of acceleration (horizontal and vertical). Another set of 2000 analyses was applied to the numerical model equally distributed between far- and near-field seismic inputs with a range of PGA between 0.45 g and 0.8 g. For this assessment, it was also required to define 125 three-component artificial accelerograms together with 125 uncertain parameters related to the mechanical properties. The time history analyses were conducted using the automatic routine considering the new variability of artificial accelerogram. This evaluation was also focused on the out-of-plane response of the main gable wall, assuming a proper connection with the return walls. Therefore, the response of the return walls was

neglected when assessing the seismic vulnerability of the brick masonry structure. Again, the dynamic response in terms of history of horizontal displacements at the top of the gable wall has been evaluated by means of the CD in order to determine the number of exceeding events for each of the LSs.

Figure 13 reports the displacement histories of the three control nodes together with the CD of the different LSs due to the application of three-component artificial accelerograms. It can be evidenced that this multi-directional approach is a powerful tool since it allows the evaluation of the different control nodes with respect to the different LSs. It can be noted that the response of this typology of structure does not only experience displacement in the Y direction (main gable wall), but also in the X direction (return walls) due to the additional component of acceleration. This response is mainly associated with the geometrical characteristics of this structure (U-shape configuration) that implies that the two unconstrained return walls experience an important out-of-plane response. Nonetheless, in this study, the seismic vulnerability assessment was conducted considering only the dynamic response associated with the gable wall and its out-of-plane response, coherently with the experimental campaign. This assumption was also based on the fact that in actual buildings, the return walls are restrained by additional structural elements which limit the out-of-plane response at the corners. After the evaluation of the dynamic response associated with a single control node, it was possible to determine the number of exceeding events which are summarized in Table 5.

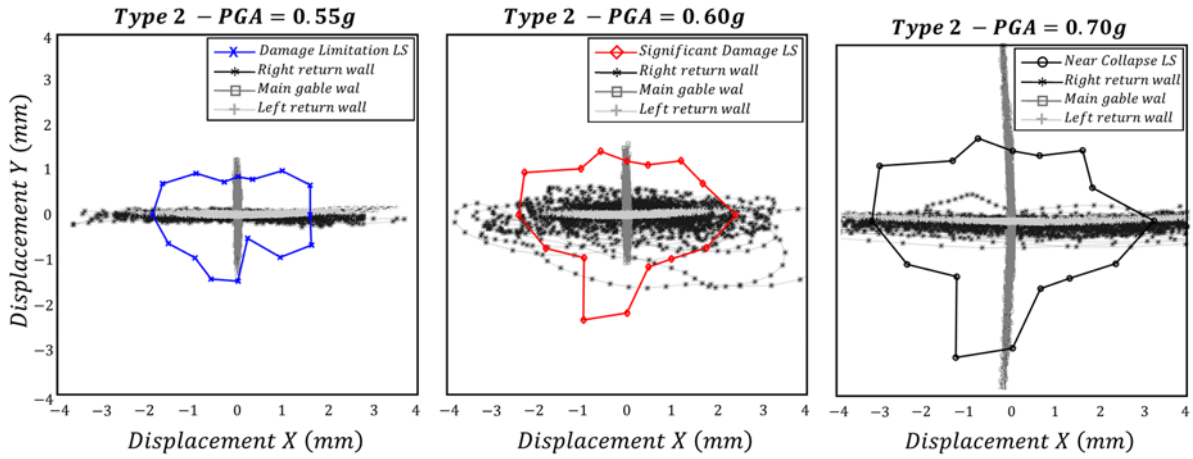

Figure 13. Assessment of seismic performance based on a Capacity Dominium due to the application of three-component artificial accelerograms: (a) Damage Limitation , (b) Significant Damage, and (c) Near Collapse LSs.

731

Table 5. Exceeding events for the derivation of analytical fragility curves due to the application of three-component artificial accelerograms (out of a set of 125).

IM	Number of events	Number of exceeding events					
		Damage Limitation LS		Significant Damage LS		Near Collapse LS	
		Type 1	Type 2	Type 1	Type 2	Type 1	Type 2
0.45 g	125	79	72	57	38	43	21
0.50 g	125	104	99	85	70	67	43
0.55 g	125	113	108	104	92	89	74
0.60 g	125	121	117	116	108	107	97
0.65 g	125	124	125	123	118	119	111
0.70 g	125	125	125	124	124	122	120
0.75 g	125	125	125	125	124	124	122
0.80 g	125	125	125	125	125	125	124

732 The fragility curves derived from the application of far- and near-field
733 three-component seismic inputs are depicted in Figure 14. In the case of far-field
734 seismic input (see solid lines in Figure 14), the occurrence of an event with an
735 intensity of 0.50 g leads to probabilities of exceedance of 82%, 68% and 58% for the
736 Damage Limitation, Significant Damage and Near Collapse LSs, respectively. It
737 can also be noted that the fragility curves are relatively close, especially when
738 considering the last two LSs. This behavior was also evidenced when assessing the
739 seismic vulnerability of the structure subjected to uniaxial inputs. The results
740 associated with the application of near-field seismic inputs are depicted in Figure
741 14 (dashed lines). In this case, the probabilities of exceeding the three LSs
742 correspond to 77%, 54% and 36% for an intensity of 0.50 g. As for the uniaxial
743 input, there is a reduction of probability when comparing the probabilities

associated with near- and far-field seismic inputs. The Damage Limitation and Near Collapse LSs presented the lowest and highest reductions of approximately 5% and 22%, respectively. Another comparison can be conducted considering the probability of exceedance of the different LSs when applying uniaxial and three-component artificial accelerograms. The probability of exceedance increased between 1.9 and 2.7 times for a far-field seismic input with an intensity of 0.50 g. In the case of near-field seismic input, the application of three-component artificial accelerograms with a PGA of 0.50 g led to an amplification of the probabilities ranging between 1.84 and 3.35 times the ones obtained with uniaxial accelerograms.

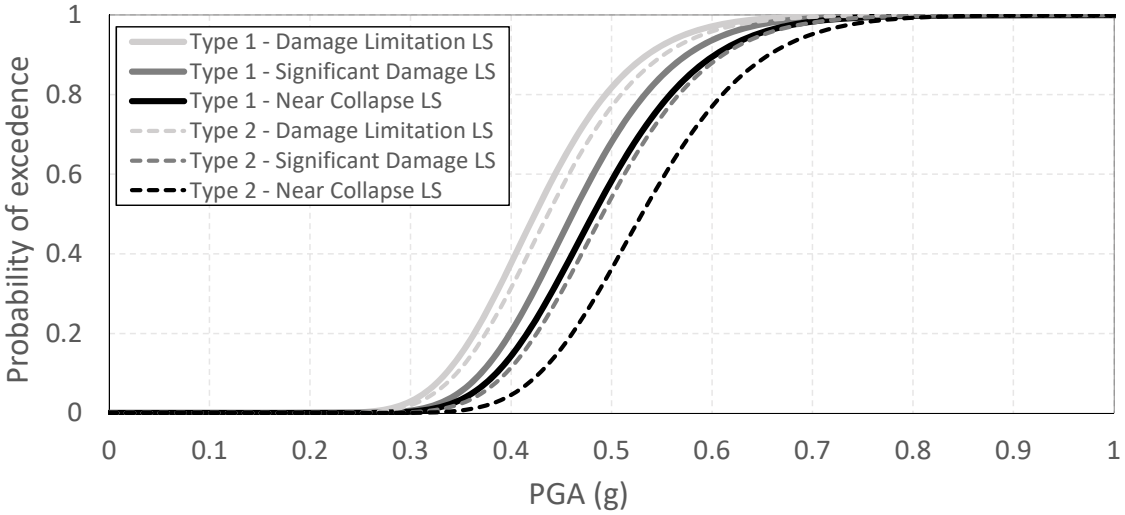

Figure 14. Analytical fragility curves derived due to the application of three-component artificial accelerograms.

5. Comparison between fragility curves

The last part of this investigation provides a comparison between fragility curves obtained by means of the proposed analytical approach and an expert-based formulation. For this purpose, the expert-based fragility functions provided by Hazus [23], for the building typology denoted as URML, is considered. URML typology corresponds to URM buildings composed by low-height bearing walls with one or two stories which somehow resemblance to the case study of this investigation. The comparison between analytical and expert-based fragility functions also required the definition of three equivalent LSs. The first LS,

763 denoted as Slight Damage, is related to diagonal and stair-step cracking on
764 masonry walls and around openings. The second one, denoted as Moderate
765 Damage, involves the occurrence of diagonal cracking in almost all masonry wall
766 and visible separation from diaphragms. The third LS, denoted as Extensive
767 Damage, consists of extensive damage in most masonry walls and overturning of
768 parapets and gable wall ends. Hazus [23] also provides a set of seismic design
769 levels for the vulnerability assessment of different building typologies, as a
770 function of the date of design and seismic hazard. The Low-code seismic design
771 level was chosen for this comparison (early design codes and moderate seismicity).
772 This comparison involved the definition of single analytical fragility curves
773 for the LSs selected for far- and near-field seismic inputs. For this purpose, an
774 additional round of fitting procedures was conducted considering the total number
775 of exceeding events as the summation of the ones obtained with uniaxial and
776 triaxial accelerograms. The characteristics of the new analytical fragility curves,
777 together with the expert-based ones, are reported in Table 6. Significant
778 differences were clearly identified when comparing the characteristics of the
779 fragility functions based on these two different formulations. The analytical mean
780 values are significantly higher than the ones provided by expert-based formulation
781 regardless of the corresponding equivalent LS. These differences can also be
782 clearly noticed in Figure 15 which shows the fragility curves provided by Hazus
783 [23] together with envelopes of far- and near-field analytical fragility curves. This
784 figure shows that URML structures reach the different LSs when subjected to a
785 lower intensity of seismic input when compared to the analytical envelopes. It can
786 be observed that the occurrence of a seismic event with an intensity of 0.50 g leads
787 to high probabilities of exceedance. In the case of the Slight Damage LS, this
788 probability corresponds to 98%, whereas for the Moderate and Extensive Damage
789 LSs, these values are 92% and 76%, respectively. This comparison demonstrates
790 how the blind use of generic approaches to defining seismic loss of URM structures
791 can provide unrealistic estimates. In addition, it also stresses the necessity of
792 conducting further and more detailed investigations regarding this topic.

Table 6. Mean value and standard deviation associated with analytical and expert-based fragility curves.

EC8-Part3 Limit states	Far -field earthquake		Near-field earthquake		Hazus [23] Limit state	Equivalent PGA Low-code seismic design level	
	θ	B	θ	B		θ	β
Damage Limitation	0.46	0.23	0.47	0.24	Slight Damage	0.14	0.64
Significant Damage	0.50	0.25	0.53	0.23	Moderate Damage	0.20	0.64
Near Collapse	0.53	0.26	0.58	0.23	Extensive Damage	0.32	0.64

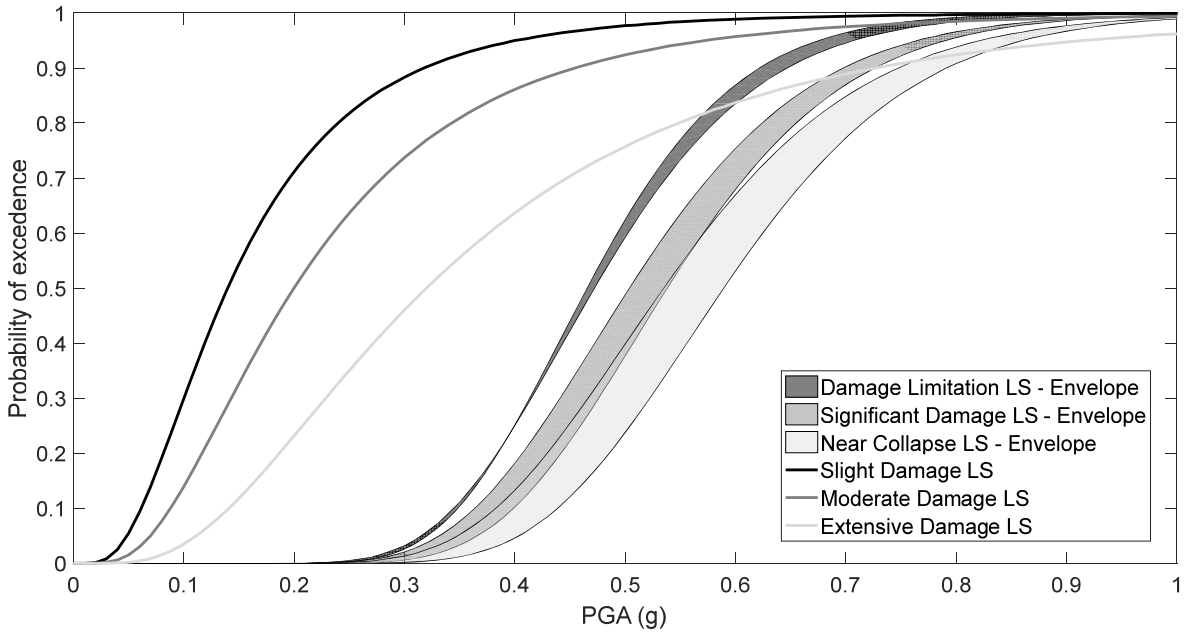

Figure 15. Comparison between analytical and expert-based fragility curves.

6. Final considerations

This paper presented a methodology for assessing the seismic vulnerability of masonry structures characterized by predominant out-of-plane failure mechanisms by means of analytical fragility curves. Such methodology involves the use of an efficient DMEM approach capable of simulating in-plane and out-of-plane mechanisms with a low computational demand. In addition, the proposed methodology is constituted by a series of thorough procedures associated with the definition of seismic input, the definition of limit states and displacement capacities, and the derivation and fitting of analytical fragility curves. Due to the advantages of the adopted modelling approach, the seismic vulnerability assessment involved the application of time history analyses, and it required the

805 definition of suitable seismic input. In addition, the limit states have been defined
806 following specifications provided by standards. Nevertheless, the definition of
807 their corresponding displacement capacity was conducted by means of an
808 alternative procedure, denoted as *Capacity Dominium*, based on multi-directional
809 pushover analyses aiming at a global assessment of structural response. Finally,
810 the derived fragility curves were subjected to a fitting process considering a
811 maximum likelihood approach.

812 In the present study, this methodology has been validated by an initial
813 application to a brick masonry structure which was experimentally and
814 numerically investigated. The generation of the seismic input was conducted
815 based on Type 1 and Type 2 elastic response spectra. Three LSs, namely Damage
816 Limitation, Significant Damage and Near Collapse, were taken into consideration
817 whose capacities were expressed in terms of horizontal top displacements of the
818 main gable wall. These displacements were defined by means of a CD obtained by
819 applying pushover analyses with an incremental angular step of 22.5°.

820 The seismic vulnerability assessment of the brick masonry structure
821 involved two main sources of uncertainty. Such uncertainty was focused on the
822 seismic input as well as the mechanical properties and geometrical properties of
823 the structure. The artificial accelerograms were subjected to eight scaling factors
824 between 0.45 and 0.80, with an incremental step of 0.05. A maximum likelihood
825 procedure was considered for the fitting of the analytical fragility curves allowing
826 the estimation of the probability of exceedance in accordance with the different
827 LSs. This approach required the definition of the actual number of exceeding
828 events which was determined by the use of the CD. Analytical fragility curves
829 associated with the application of far and near-field seismic inputs were derived
830 using the DME model of the brick masonry structure. These results demonstrated
831 the capability of the proposed modeling approach for performing sophisticated
832 analyses for practical applications.

833 In particular, for the analyzed structure, an important difference was
834 found between uniaxial and triaxial seismic input: on average, considering all
835 Limit States and a probability of exceedance of 50%, a 19% reduction of the PGA
836 input is found when comparing the triaxial and the uniaxial seismic inputs.

Additionally, the comparison between analytical and expert-based formulations showed some marked differences in terms of fragility curves and their corresponding probabilities of exceedance. Therefore, it is necessary to carefully apply expert-based formulations for a specific location and structural typology, and further investigations associated with the seismic vulnerability of URM structures are required. The definition of a more rigorous procedure for the estimation of the displacement capacity, suitable in a dynamic context and that involves in-plane and out-of-plane mechanisms, constitutes an important task that needs to be investigated in future.

In general, it is important to notice that the main steps in this methodology, namely, application of multidirectional pushover analyses for the definition of the displacement capacity as well as nonlinear dynamic analyses for the derivation of fragility curves, require a reasonable computational burden. The analysis demand required for this type of assessment may constitute an important limitation of this methodology; however, it is significantly low when compared to sophisticated and refined FE numerical models characterized by a large number of DOFs. As previously stated, the application of a single nonlinear dynamic analysis was characterized by an average duration of 30 minutes. For this reason, the authors believe that the proposed methodology may allow a thorough assessment of the seismic vulnerability of URM structures.

7. Acknowledgment

The first author gratefully acknowledges the financial support of the Peruvian Institution Innovate Perú/FINCyT (Fondo para la Innovación, Ciencia y Tecnología) through the PhD grant BECA-1-P-078-13. The first author acknowledge the support and helpful advices provided by Dr. Helder Sousa from the University of Minho.

8. References

[1] P. G. Asteris, A. Moropoulou, A. D. Skentou, M. Apostolopoulou, A. Mohebkhah, L. Cavaleri, H. Rodrigues, and H. Varum, "Stochastic Vulnerability Assessment of

Masonry Structures: Concepts, Modeling and Restoration Aspects," *Applied Sciences,* vol. 9, p. 243, (2019).

[2] B. R. Ellingwood, "Earthquake risk assessment of building structures," *Reliability Engineering & System Safety,* vol. 74, pp. 251-62, (2001).

[3] T. Rossetto and A. Elnashai, "Derivation of vulnerability functions for European-type RC structures based on observational data," *Engineering Structures,* vol. 25, pp. 1241-63, (2003). doi: 10.1016/S0141-0296(03)00060-9

[4] *ATC-13, Earthquake damage evaluation data for California,* Applied technology council FEMA contract no. EMW-C-0912, 1985.

[5] M. Rota, A. Penna, and C. L. Strobbia, "Processing Italian damage data to derive typological fragility curves," *Soil Dynamics and Earthquake Engineering,* vol. 28, pp. 933–947, (2008).

[6] M. Rota, "Advances in the derivation of fragility curves for masonry buildings," PhD thesis, European School for Advanced Studies in Reduction of Seismic Risk (ROSE School), Pavia, Italy, (2007).

[7] *ATC, FEMA-273: NEHRP Guidelines for the seismic rehabilitation of buildings. Basic procedures manual,* Applied Technology Council (ATC), 1997.

[8] *ATC, FEMA-306: Evaluation of earthquake damaged concrete and masonry wall buildings. Basic Procedures Manual,* Applied Technology Council (ATC), 1998.

[9] *Eurocode 8: Design of structures for earthquake resistance – Part 3: General rules, seismic actions and rules for buildings, Design Code EN 1998-3*, 2005.

[10] *NZSEE: Assessment and improvement of the structural performance of buildings in earthquakes. New Zealand Society of Earthquake Engineering.,* University of Auckland, 2006.

[11] *NTC 2008, Decreto Ministeriale 14/1/2008: Norme tecniche per le costruzioni.,* Ministry of Infrastructures and Transportations, 2008.

[12] G. M. Calvi, "A displacement-based approach for vulnerability evaluation of classes of buildings," *Journal of Earthquake Engineering,* vol. 3, pp. 411-38, (1999).

[13] A. J. Kappos, G. Panagopoulos, C. Panagiotopoulos, and G. Penelis, "A hybrid method for the vulnerability assessment of R/C and URM buildings.," *Bulletin of Earthquake Engineering,* vol. 4, pp. 421-44, (2006).

[14] P. G. Asteris, "On the structural analysis and seismic protection of historical masonry structures," *The Open Construction and Building Technology Journal,* vol. 2, pp. 124-33, (2008).

[15] A. Mouyiannou, M. Rota, A. Penna, and G. Magenes, "Identification of suitable limit states for nonlinear dynamic analyses of masonry structures," *Journal of Earthquake Engineering,* vol. 18, pp. 231-63, (2014).

[16] S. Petry and K. Beyer, "Influence of boundary conditions and size effect on the drift capacity of URM walls," *Engineering Structures,* vol. 65, pp. 76-88, (2014).

[17] S. Lagomarsino and S. Cattari, "Seismic performance of historical masonry structures through pushover and nonlinear dynamic analyses," in *Perspectives on European Earthquake Engineering and Seismology*, Springer, (2015), pp. 265-292.

[18] S. Lagomarsino and S. Cattari, "PERPETUATE guidelines for seismic performance-based assessment of cultural heritage masonry structures," *Bulletin of Earthquake Engineering,* vol. 13, pp. 13-47, (2015). doi: 10.1007/s10518-014-9674-1

[19] M. Rota, A. Penna, and G. Magenes, "A methodology for deriving analytical fragility curves for masonry buildings based on stochastic nonlinear analyses," *Engineering Structures,* vol. 32, pp. 1312-23, (2010).

[20] G. Grünthal, "European macroseismic scale 1998 (EMS 1998). Council of Europe, Cahiers du Centre Europe´en de Géodynamique et de Sismologie," p. 15.

[21] B. Omidvar, B. Gatmiri, and S. Derakhshan, "Experimental vulnerability curves for the residential buildings of Iran," *Natural Hazards,* vol. 60, pp. 345–365, (2012). doi: 10.1007/s11069-011-0019-y

[22] J. Park, P. Towashiraporn, J. I. Craig, and B. J. Goodno, "Seismic fragility analysis of low-rise unreinforced masonry structures," *Engineering Structures,* vol. 2009, pp. 125-37, (2009).

[23] *HAZUS 99 earthquake loss estimation methodology, technical manual,* N.-N. I. o. B. Science, 1999.

[24] L. Pasticier, C. Amadio, and M. Fragiacomo, "Non-linear seismic analysis and vulnerability evaluation of a masonry building by means of the SAP2000 V.10 code," *Earthquake Engineering & Structural Dynamics,* vol. 37, pp. 467–485, (2008).

[25] CSI (Computers and Structures Inc.), "SAP2000 v10 Integrated Finite Element Analysis and Design of Structures," (2004), Berkeley,

[26] P. G. Asteris, M. G. Douvika, M. Apostolopoulou, and A. Moropoulou, "Seismic and Restoration Assessment of Monumental Masonry Structures," *Materials,* vol. 10, p. 895, (2017).

[27] M. Apostolopoulou, E. Aggelakopoulou, L. Siouta, A. Bakolas, M. G. Douvika, P. G. Asteris, and A. Moropoulou, "A methodological approach for the selection of compatible and performable restoration mortars in seismic hazard areas," *Construction and Building Materials,* vol. 155, pp. 1-14, (2017).

[28] P. G. Asteris, M. P. Chronopoulos, C. Z. Chrysostomou, H. Varum, V. Plevris, N. Kyriakides, and V. Silva, "Seismic vulnerability assessment of historical masonry structural systems," *Engineering Structures,* vol. 62-63, pp. 118-134, (2014).

[29] S. Lagomarsino, A. Penna, A. Galasco, and S. Cattari, "TREMURI program: An equivalent frame model for the nonlinear seismic analysis of masonry buildings," *Engineering Structures,* vol. 56, pp. 1787-1799, (2013).

[30] M. A. Erberik, "Generation of fragility curves for Turkish masonry buildings considering in-plane failure modes," *Earthquake Engineering & Structural Dynamics,* vol. 37, pp. 387-405, (2008).

[31] Y. Mengi, H. D. McNiven, and A. D. Tanrıkulu, "Models for nonlinear earthquake analysis of brick masonry buildings.," University of California at Berkeley(1992).

[32] D. D'Ayala, "Force and displacement based vulnerability assessment for traditional buildings," *Bulletin of Earthquake Engineering* vol. 3, pp. 235-65, (2005).

[33] S. Cattari, S. Frumento, S. Lagomarsino, S. Parodi, and S. Resemini, "Multi-level procedure for the seismic vulnerability assessment of masonry buildings: The case of Sanremo (north-western italy)," in *1st European Conference on Earthquake Engineering and Seismology (ECEES)*, Geneva, Switzerland (2006).

[34] G. Milani and G. Venturini, "Automatic fragility curve evaluation of masonry churches accounting for partial collapses by means of 3D FE homogenized limit analysis," *Computers and Structures,* vol. 89, pp. 1628-1648, (2011).

[35] I. Caliò, M. Marletta, and B. Pantò, "A new discrete element model for the evaluation of the seismic behaviour of unreinforced masonry buildings," *Engineering Structures,* vol. 40, pp. 237-338, (2012).

[36] B. Pantò, F. Cannizzaro, I. Caliò, and P. B. Lourenço, "Numerical and experimental validation of a 3D macro-model for the in-plane and out-of-plane behaviour of unreinforced masonry walls," *International Journal of Architectural Heritage,* (2017). doi: 10.1080/15583058.2017.1325539

[37] T. Takeda, M. A. Sozen, and N. N. Nielsen, "Reinforced concrete response to simulated earthquakes," *Journal of the Structural Division,* vol. 96, pp. 2557-2573, (1970).

[38] V. Turnsek and F. Cacovic, "Some experimental result on the strength of brick masonry walls," in *2nd International Brick Masonry Conference*, Stoke-on-Trent, UK (1971).
[39] C. Chácara, F. Cannizzaro, B. Pantò, I. Caliò, and P. B. Lourenço, "Assessment of the Dynamic Response of Unreinforced Masonry Structures using a Macro-Element Modelling Approach," *Earthquake Engineering and Structural Dynamics,* vol. 47, pp. 2426-46, (2018).
[40] HISTRA s.r.l, "HiStrA (Historical Structure Analysis) Release 17.2.3," ed. Catania, Italy, (2015.
[41] F. Cannizzaro, B. Pantò, M. Lepidi, S. Caddemi, and I. Caliò, "Multi-directional seismic assessment of historical masonry buildings by means of macro-element model-ling: Application to a building damaged during the L'Aquila earthquake (Italy)," *Buildings,* vol. 7, (2017).
[42] J. W. Baker, "Efficient Analytical Fragility Function Fitting Using Dynamic Structural Analysis," *Earthquake Spectra,* vol. 31, pp. 579-99, (2015).
[43] P. X. Candeias, A. Campos Costa, N. Mendes, A. A. Costa, and P. B. Lourenço, "Experimental Assessment of the Out-of-Plane Performance of Masonry Buildings Through Shaking Table Tests," *International Journal of Architectural Heritage,* vol. 11, pp. 31-58, (2017).
[44] TNO, "DIANA - DIsplacement method ANAlyser," (2018), Delft, Netherlands,
[45] *Eurocode 8: Design of structures for earthquake resistance – Part 1: General rules, seismic actions and rules for buildings, EN 1998-1*, 2004.
[46] *NP EN 196-8, Eurocode 8: Design of structures for earthquake resistance Part 1: General rules, seismic actions and rules for buildings -Portuguese Institute for Quality*, 2010.
[47] D. A. Gasparini and E. H. Vanmarcke, "SIMQKE, A Program for Artificial Motion Generation: User's Manual and Documentation," (1976), Department of Civil Engineering, MIT, USA,
[48] L. Mendes, "LNEC-SPA: Signal Processing and Analysis Tools for Civil Engineers," Lisbon, Portugal Patent, 2008.
[49] B. Pantò, F. Cannizzaro, S. Caddemi, I. Caliò, C. Chácara, and P. B. Lourenço, "Nonlinear Modelling of Curved Masonry Structures after Seismic Retrofit through FRP Reinforcing," *Buildings,* vol. 7, p. 79, (2017). doi: 10.3390/buildings7030079
[50] P. B. Lourenço, "Recent advances in masonry modelling : Micromodelling and homogenisation," in *Multiscale modeling in solid mechanics: Computational approaches*, U. Galvanetto and M. H. Ferri Aliabadi, London, UK, (2009.
[51] *JCSS Probability Model Code Part 3: Resistance Models,* Joint Committee of Structural Safety, 2011.
[52] C. Chácara, P. B. Lourenço, B. Pantò, F. Cannizzaro, and I. Caliò, "Macro-Element Mass Matrix for the Dynamic Assessment of Unreinforced Masonry Structures," in *Congreso de Métodos Numéricos en Ingeniería*, Valencia, Spain (2017).